

Interplay between hard and soft processes in HYDJET++ model

E.E. Zabrodin*

Department of Physics, University of Oslo, Oslo, Norway

Skobel'tzyn Institute of Nuclear Physics, Moscow State University, Moscow, Russia

*National Research Nuclear University "MEPhI" (Moscow Engineering Physics Institute),
Moscow, Russia*

E-mail: eugen.zabrodin@fys.uio.no

L.V. Bravina

Department of Physics, University of Oslo, Oslo, Norway

G.Kh. Eyyubova, I.P. Lokhtin, L.V. Malinina, S.V. Petrushanko, A.M. Snigirev

Skobel'tzyn Institute of Nuclear Physics, Moscow State University, Moscow, Russia

The Monte Carlo event generator HYDJET++ (HYDrodynamics with JETs) contains the description of both soft and hard processes in relativistic heavy-ion collisions by combining the parametrized hydrodynamics with the treatment of jets. The interplay of hard and soft processes describes the violation of the mass hierarchy of meson and baryon elliptic (v_2) and triangular (v_3) flows at intermediate transverse momenta, the fall-off of the flow harmonics after the certain p_T threshold, and the worsening of the number-of-constituent-quark (NCQ) scaling of v_2 and v_3 at LHC energies compared to that at RHIC ones. The role of this interplay in di-hadron correlations and in production of open and hidden charm in heavy-ion collisions at RHIC and LHC energies is also discussed.

High- p_T Physics at RHIC and LHC era

October 2 - 5 2017

Bergen, Norway

*Speaker.

1. Introduction

HYDJET++ [1] is one of the models included in the event generator pool of CMS Collaboration. It combines the treatment of soft processes with the description of jets propagating in hot and dense partonic medium. The simulation of both soft and hard processes proceeds almost independently. The soft processes are generated by the FASTMC model [2, 3] which employs the parametrized hydrodynamics extended to non-central nuclear collisions to provide elliptic, v_2 , triangular, v_3 , and higher harmonics, v_n , $n > 3$, of the anisotropic flow. Recall, that the flow harmonics are the coefficients of the Fourier series expansion of azimuthal particle distribution in the transverse plane,

$$v_n = \langle \cos [n(\phi - \Psi_n)] \rangle \quad (1.1)$$

Here ϕ is the particle azimuthal angle, and Ψ_n is the azimuth of the event plane of n -th harmonic, respectively. Averaging in Eq.(1.1) is performed over all hadrons in an event and over all events.

At any given impact parameter b the program calculates first the number of participating nucleons which permits one to estimate the effective volume V_{eff} of the overlapping zone. Then, the fireball expansion is governed by Bjorken hydrodynamics. When the temperature drops below a certain threshold value, which is a free parameter of the model, the chemical freeze-out of the system takes place. The fireball continues to expand further until the stage of thermal freeze-out. HYDJET++ is flexible in a sense that it allows also for a scheme with simultaneous chemical and thermal freeze-out. However, the best agreement with the experimental data is obtained in the scenario with two separated freeze-outs. Final-state interactions are represented by two- and three-body decays of resonances. The table of particles and resonances in HYDJET++ is very rich; it contains more than 360 baryonic and mesonic states including the charmed ones.

Hard processes in HYDJET++ are handled by the routine PYQUEN (PYTHIA QUENched) [4]. It takes into account both collisional and radiational energy losses experienced by hard partons in hot and dense medium. The number of hard jets in A+A collisions at a given impact parameter is determined by the number of binary nucleon-nucleon (NN) collisions and the integral cross section of the hard NN collision with certain minimum transverse momentum transfer p_T^{min} . Compared to its original version [1], which took into account just elliptic flow [5, 6], the model was further upgraded to (i) better treatment of the hard processes at LHC energies by replacement of standard PYTHIA 6.4 to Pro-Q20 tune [7], (ii) triangular flow [8, 9, 10] and, consequently, higher flow harmonics up to hexagonal flow [11, 12], and (iii) event-by-event fluctuations of the flow harmonics [13]. The anisotropic flow in HYDJET++ arises because of two reasons, namely, spatial (or geometric) anisotropy of the fireball and dynamical (or flow momentum) anisotropy.

In case of spatial elliptic eccentricity of the fireball its radius reads

$$R_2(b, \phi) = R_{fr} \left\{ \frac{1 - \varepsilon_2^2(b)}{1 + \varepsilon_2^2(b) \cos [2(\phi - \Psi_2)]} \right\}^{1/2}, \quad (1.2)$$

where Ψ_2 is the azimuth of the event plane of elliptic flow and ε_2^2 is a free parameter of the model. It links the freeze-out radius of the fireball $R_{fr}(b)$ in a non-central collision to that of a central one $R_{fr}(b=0) \equiv R_0$ as $R_{fr}(b=0) = R_0 \sqrt{1 - \varepsilon_2^2(b)}$. To create spatial triangularity, Eq.(1.2) should be

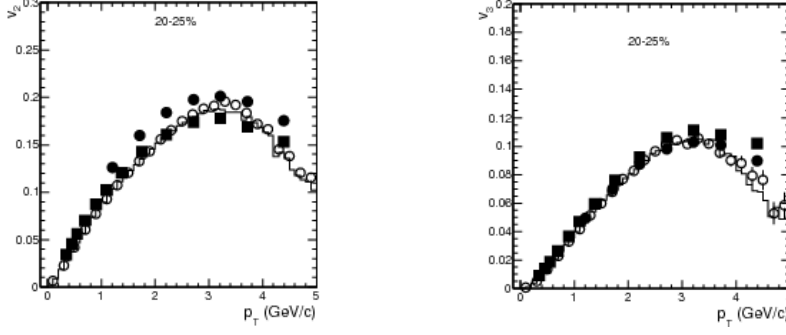


Figure 1: Differential (a) elliptic and (b) triangular flow of charged hadrons in Pb+Pb collisions with centrality 20 – 25% at $\sqrt{s} = 2.76$ TeV. Solid symbols are data from [15], open circles and histogram are HYDJET++ calculations, respectively.

modified further [8]

$$R_3(b, \phi) = R_2(b, \phi) \{1 + \varepsilon_3(b) \cos[3(\phi - \Psi_3)]\} , \quad (1.3)$$

containing the azimuth of the event plane of triangular flow, Ψ_3 , and the new free parameter, $\varepsilon_3(b)$, responsible for generation of triangular profile of the freeze-out hypersurface. Experiments show that elliptic and triangular flows are not correlated, therefore, their azimuths are randomly distributed in HYDJET++. Note also, that both $\varepsilon_2(b)$ and $\varepsilon_3(b)$ are normally distributed at any impact parameter around their mean values to account for initial state fluctuations [13]. Therefore, the spatial anisotropies may arise in collisions with $b = 0$ as well.

Another source of the anisotropic flow is the dynamical anisotropy. It originates from non-zero angle between the collective flow velocity of the fluid cell ϕ_{cell} and direction of the radius-vector

$$\tan \phi_{\text{cell}} = \sqrt{\frac{1 - \delta_2(b)}{1 + \delta_2(b)}} \tan \phi , \quad (1.4)$$

where $\delta_2(b)$ is another free parameter responsible for formation of v_2 . To diminish the number of free parameters to be fitted at all centralities, HYDJET++ employs the relation between the v_2 , ε_2 , and δ_2 obtained within the hydrodynamic approach in [14]

$$v_2(\varepsilon_2, \delta_2) \propto \frac{2(\delta_2 - \varepsilon_2)}{(1 - \delta_2^2)(1 - \varepsilon_2^2)} . \quad (1.5)$$

This approximation provides fair results up to centrality $\sigma/\sigma_{\text{geo}} \leq 40 - 45\%$. At more peripheral events one has to treat $\delta_2(b)$ and $\varepsilon_2(b)$ completely independently. The last free parameter responsible for the triangular momentum anisotropy is denoted as $\rho_3(b)$. Further details of the model can be found in [1, 7, 13] and references therein.

2. Interplay of hard and soft processes.

Influence of the interplay on differential elliptic and triangular flows. To see this influence explicitly, we display in Fig. 1(a,b) two distributions, $v_2^{\text{ch}}(p_T)$ and $v_3^{\text{ch}}(p_T)$, obtained in HYDJET++

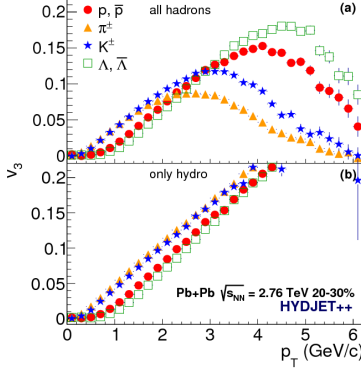


Figure 2: Differential triangular flow of identified hadrons in (a) all processes and (b) only in hydrodynamics in Pb+Pb collisions at 2.76 TeV with centrality 20 – 30%.

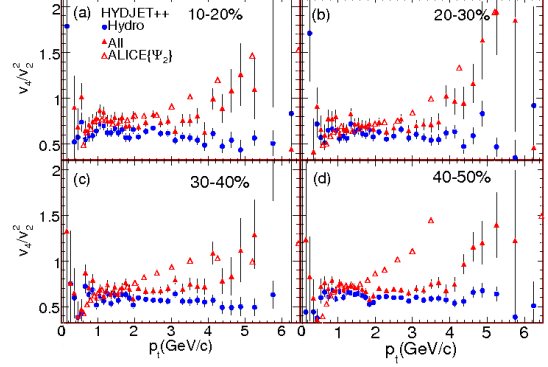


Figure 3: Ratio v_4/v_2^2 vs p_T for charged hadrons in Pb+Pb collisions at 2.76 TeV with different centralities with (\blacktriangle) and without jets (\bullet) compared to ALICE data [17] (\triangle).

calculations of Pb+Pb collisions with centrality 20 – 25% at $\sqrt{s} = 2.76$ TeV. It is well-known that in ideal hydrodynamics both elliptic and triangular flow increases with rising transverse momentum. The differential flows in Fig. 1, however, drop at $p_T \geq 2.5$ GeV/c. - The collective flow is carried by hadrons produced in soft processes, whereas the flow of hadrons decoupled from jets is essentially zero. Jet particles can develop a weak flow at $p_T \geq 3.5$ GeV/c because of the jet quenching. Spectrum of hadrons is dominated by particles from the hydro-like processes at $p_T \leq 2$ GeV/c, and by jet particles at $p_T \geq 3$ GeV/c. Therefore, the elliptic or triangular flow of the combined soft+hard hadron spectrum drops after a certain transverse momentum. For light hadrons the crossing of the soft and hard parts of their p_T -spectra occurs at smaller transverse momenta compared to those of heavy hadrons. This explains naturally the violation of the mass hierarchy of differential flows (lighter hadrons have larger flow in a low- p_T region) and crossing of the meson and baryon flows somewhere at intermediate p_T . Both features are seen in Fig. 2, which shows the differential triangular flow of identified hadrons for the combined soft+hard spectrum, and only for hadrons coming from hydro processes.

Jets and violation of scaling ratios. It was a hint that the ratios $v_n^{1/n}(p_T)/v_2^{1/2}(p_T)$ should be almost independent on the transverse momenta. Experimental results seem to confirm this hypothesis [16]. In Fig. 3 we plot the ratio v_4/v_2^2 as a function of transverse momentum for four different centralities in Pb+Pb collisions at $\sqrt{s} = 2.76$ TeV. The ALICE data show that the ratio increases at $p_T \geq 3$ GeV/c. HYDJET++ calculations with and without jets indicate that the increase emerges because of the contributions from the hard processes.

Jets are also responsible for violation of the number-of-constituent-quark (NCQ) scaling of both v_2 and v_3 . To observe this scaling one has to divide the flow of a hadronic specie and the transverse kinetic energy $KE_T = m_T - m_0$ by the number of constituent quarks, 2 for mesons and 3 for baryons. Figures 4 and 5 display that both for elliptic (Fig. 4) and for triangular (Fig. 5) flow the decays of resonances modify the spectra towards the fulfillment of the NCQ scaling. In contrast, because of the jet influence the scaling fulfillment gets worse.

Violation of factorization of dihadron angular harmonics. Here the azimuthal distribution of

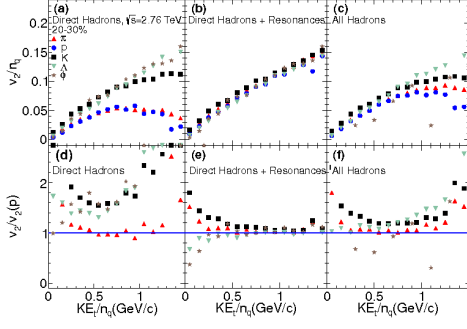


Figure 4: The KE_T/n_q dependence of the elliptic flow of direct hadrons (left), all hadrons produced only in soft processes (middle), and all hadrons (right) in Pb+Pb collisions at 2.76 TeV with centrality 20 – 30%.

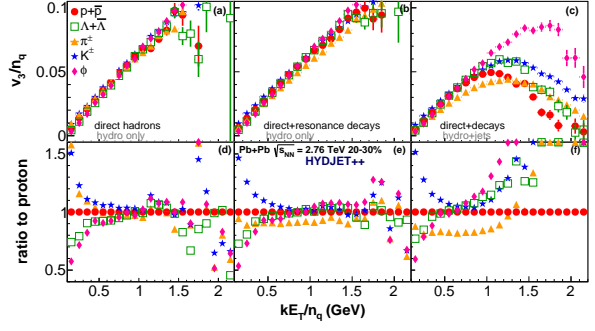


Figure 5: The same as Fig.4 but for the triangular flow. Here only hadrons directly produced in soft processes are considered in left windows.

two particles, denoted as the “trigger” and the “associated” ones, is expanded in a Fourier series

$$\frac{dN^{pairs}}{d\Delta\phi} \propto 1 + 2 \sum_{n=2}^{\infty} v_n(p_T^{tr}) v_n(p_T^a) \cos(n\Delta\phi), \quad (2.1)$$

where $\Delta\phi = \phi^{tr} - \phi^a$. In the flow-dominated regime, which takes place at low transverse momenta, the coefficients V_n can be presented as

$$V_n(p_T^{tr}, p_T^a) = v_n(p_T^{tr}) \times v_n(p_T^a) + \delta_n, \quad (2.2)$$

where v_n are the corresponding flow harmonics and δ_n is the contribution of non-flow processes. The calculations of v_2 , v_3 and v_4 shown in Fig. 6 reveal that factorization $V_n = v_n^{tr} \times v_n^a$ works well at $p_T \leq 3$ GeV/c. At higher transverse momenta the non-flow contribution δ_n from the jets dominates, and the factorization is broken (see [18] for details).

Freeze-out of charmed mesons. This problem was studied in [19]. In line with previous investigations, it seems that J/ψ -mesons are frozen earlier than the light hadrons. In contrast, for D -mesons whose p_T -spectra are displayed in Fig. 7 the simultaneous thermal freeze-out with other hadrons are not ruled out.

3. Conclusions

Interplay of hard and soft processes in relativistic heavy-ion collisions can explain many experimentally observed features, such as (i) drop of the flow harmonics at $p_T \geq 3$ GeV/c; (ii) violation of the mass hierarchy in v_2 and v_3 ; (iii) worsening of the NCQ scaling conditions for both v_2 and v_3 ; (iv) violation of factorization of di-hadron angular harmonics at $p_T \geq 3$ GeV/c. It can also shed light on thermal and non-thermal production of charmed hadrons in these reactions.

Acknowledgements. This work was supported in parts by the Russian Foundation for Basic Research under grant No. 18-02-00155 and the Norwegian Research Council (NFR) under grant No. 255253/F50 - CERN Heavy Ion Theory.

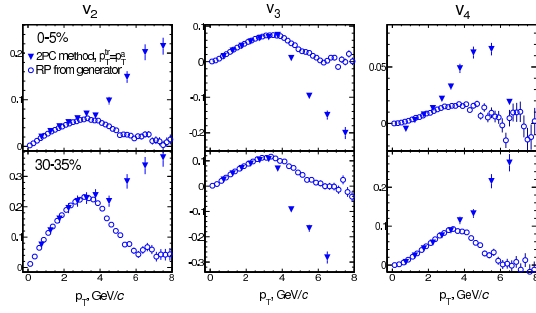


Figure 6: Single-particle flow harmonics v_n obtained directly (open circles) and extracted from V_n (solid triangles) in Pb+Pb collisions at $\sqrt{s} = 2.76$ TeV with centrality 0 – 5% (upper row) and 30 – 35% (bottom row).

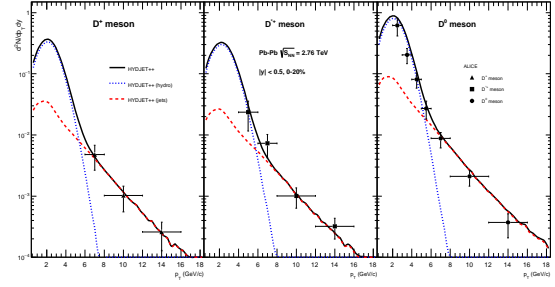


Figure 7: p_T -spectra of D^\pm (left), $D^{*\pm}$ (middle), and D^0 (right panel) at midrapidity $|y| < 0.5$ in Pb+Pb collisions at $\sqrt{s} = 2.76$ TeV with centrality 0 – 20%. Curves represent hydro (dotted), hard (dashed) and all (solid) processes, symbols denote ALICE data [20].

References

- [1] I.P. Lokhtin, L.V. Malinina, S.V. Petrushanko, A.M. Snigirev, I. Arsene, K. Tywoniuk, *Comput. Phys. Commun.* **180**, 779 (2009).
- [2] N.S. Amelin *et al.*, *Phys. Rev. C* **74**, 064901 (2006).
- [3] N.S. Amelin *et al.*, *Phys. Rev. C* **77**, 014903 (2008).
- [4] I.P. Lokhtin, A.M. Snigirev, *Eur. Phys. J. C* **45**, 211 (2006).
- [5] G. Eyyubova *et al.*, *Phys. Rev. C* **80**, 064907 (2009).
- [6] E.E. Zabrodin *et al.*, *J. Phys. G* **37**, 094060 (2010).
- [7] I.P. Lokhtin *et al.*, *Eur. Phys. J. C* **72**, 2045 (2012).
- [8] L.V. Bravina *et al.*, *Eur. Phys. J. C* **74**, 2807 (2014).
- [9] J. Crkovská *et al.*, *Phys. Rev. C* **95**, 014910 (2017).
- [10] E.E. Zabrodin *et al.*, *J. Phys.: Conf. Ser.* **668**, 012099 (2016).
- [11] L. Bravina, B.H. Bruschheim Johansson, G. Eyyubova, E. Zabrodin, *Phys. Rev. C* **87**, 034901 (2013).
- [12] L.V. Bravina *et al.*, *Phys. Rev. C* **89**, 024909 (2014).
- [13] L.V. Bravina *et al.*, *Eur. Phys. J. C* **75**, 588 (2015).
- [14] U. Wiedemann, *Phys. Rev. C* **57**, 266 (1998).
- [15] S. Chatrchyan *et al.* (CMS Collaboration), *Phys. Rev. C* **87**, 014902 (2013).
- [16] G. Aad *et al.* (ATLAS Collaboration), *Phys. Rev. C* **86**, 014907 (2012).
- [17] B. Abelev *et al.*, (ALICE Collaboration), *Phys. Lett. B* **719**, 18 (2013).
- [18] G.Kh. Eyyubova *et al.*, *Phys. Rev. C* **91**, 064907 (2015).
- [19] I.P. Lokhtin *et al.*, *J. Exp. Theor. Phys.* **124**, 244 (2017).
- [20] B. Abelev *et al.*, (ALICE Collaboration), *JHEP* **1209**, 112 (2012).